Geophysical Research Letters

RESEARCH LETTER
10.1029/2018GL080396

**Key Points:**
- Repeat sonar surveys and sedimentary provenance document sediment transport and erosion in Delgada submarine canyon, Northern California
- Hydrodynamic modeling and littoral budgets suggest that coarse sediment is mobilized by waves in the canyon head, triggering turbidity currents
- Sediment supply and wave focusing promote erosion of submarine canyons along tectonic coasts, encouraging littoral to deep sea connectivity

**Supporting Information:**
- Supporting Information S1

**Correspondence to:**
M. E. Smith,
michael.e.smith@nau.edu

**Citation:**
Smith, M. E., Werner, S. H., Buscombe, D., Finnegan, N. J., Sumner, E. J., & Mueller, E. R. (2018). Seeking the shore: Evidence for active submarine canyon head incision due to coarse sediment supply and focusing of wave energy. *Geophysical Research Letters*, *45*. https://doi.org/10.1029/2018GL080396

Received 6 SEP 2018
Accepted 10 NOV 2018
Accepted article online 14 NOV 2018



# Seeking the Shore: Evidence for Active Submarine Canyon Head Incision Due to Coarse Sediment Supply and Focusing of Wave Energy

**M. Elliot Smith[1], Samuel H. Werner[1], Daniel Buscombe[1], Noah J. Finnegan[2], Esther J. Sumner[3], and Erich R. Mueller[4]**

[1]School of Earth and Sustainability, Northern Arizona University, Flagstaff, AZ, USA, [2]Earth Sciences, University of California, Santa Cruz, CA, USA, [3]Ocean and Earth Science, University of Southampton, Southampton, UK, [4]Department of Geography, University of Wyoming, Laramie, WY, USA

**Abstract** Submarine flows carve canyons into continental shelves, yet the conditions and events responsible for canyon incision are incompletely understood. Coarse sediment flux has been shown to promote terrestrial bedrock incision via abrasion in rivers, but similar processes in submarine canyons have yet to be systematically documented. We use repeat bathymetry, provenance analysis, wave modeling, and channel network analysis to show that longshore sheltering and wave focusing by the Delgada submarine canyon induce sediment accumulation and elevated wave shear stresses in its headwall region that frequently mobilize coarse bed material. These mobilizations scour bedrock in the headwall and generate abrasive turbidity currents that work to carve the canyon's active channel into bedrock. These findings highlight an important positive feedback between submarine canyons, waves, and sediment supply and suggest that submarine canyons adjacent to wave-dominated, coarse sediment-rich coastlines *seek the shoreline* through headward incision.

**Plain Language Summary** The carving of submarine canyons into the continental shelf is poorly understood relative to river valleys on land. We studied a submarine canyon in Northern California that is connected through littoral transport to river sediment using a combination of seafloor mapping, tracking sediments using their chemical elements, and simulating waves and currents to better understand which processes are responsible for canyon erosion. Our findings suggest that canyon focusing of wave energy and an abundant supply of coarse sediment cause erosion at the canyon's head. This finding helps explain why submarine canyon channel networks erode toward shore and predicts that canyons near mountain ranges will preferentially remain connected the shoreline.

## 1. Introduction

Submarine canyons transport large quantities of terrestrial-derived sediment across the continental shelf into deep ocean basins (Covault et al., 2014; Paull et al., 2011). Density currents, for example, turbidity currents and debris flows, are responsible for shaping submarine canyons and fans, yet the conditions required and processes that control submarine headwall incision are incompletely understood (Mitchell, 2014; Parker, 1982; Shepard, 1981; Shepard & Dill, 1966; Talling, 2014). Recent analysis shows that canyon occurrence is predicted by durable onshore bedrock and high sediment supply (Smith et al., 2017), suggesting a mechanistic link between bedrock incision and the mobility of durable coarse sediment that is well documented in terrestrial settings (Cook et al., 2012; Lamb et al., 2015).

At multiple locations around the world, submarine canyon heads are displaced from direct riverine sediment input by open coasts and are fed instead by longshore transport through littoral cells (Arzola et al., 2008; Covault et al., 2011; Perg et al., 2003). Coarse sediment transport in such canyons can occur due to two primary processes: mass failure by slumping or breaching (Goldfinger et al., 2007; Mastbergen & van den Berg, 2003) and the settling of wave-generated littoral sediment plumes analogous to river-generated plumes (Hizzett et al., 2018; Paull et al., 2003).

The King Range in Northern California is the onshore manifestation of the Mendocino Triple Junction (Dickinson & Snyder, 1979; Figure 1a). Rapid Pliocene through recent uplift of the King Range can be attributed to transpression along a major left step where San Andreas Fault displacement is transferred to the

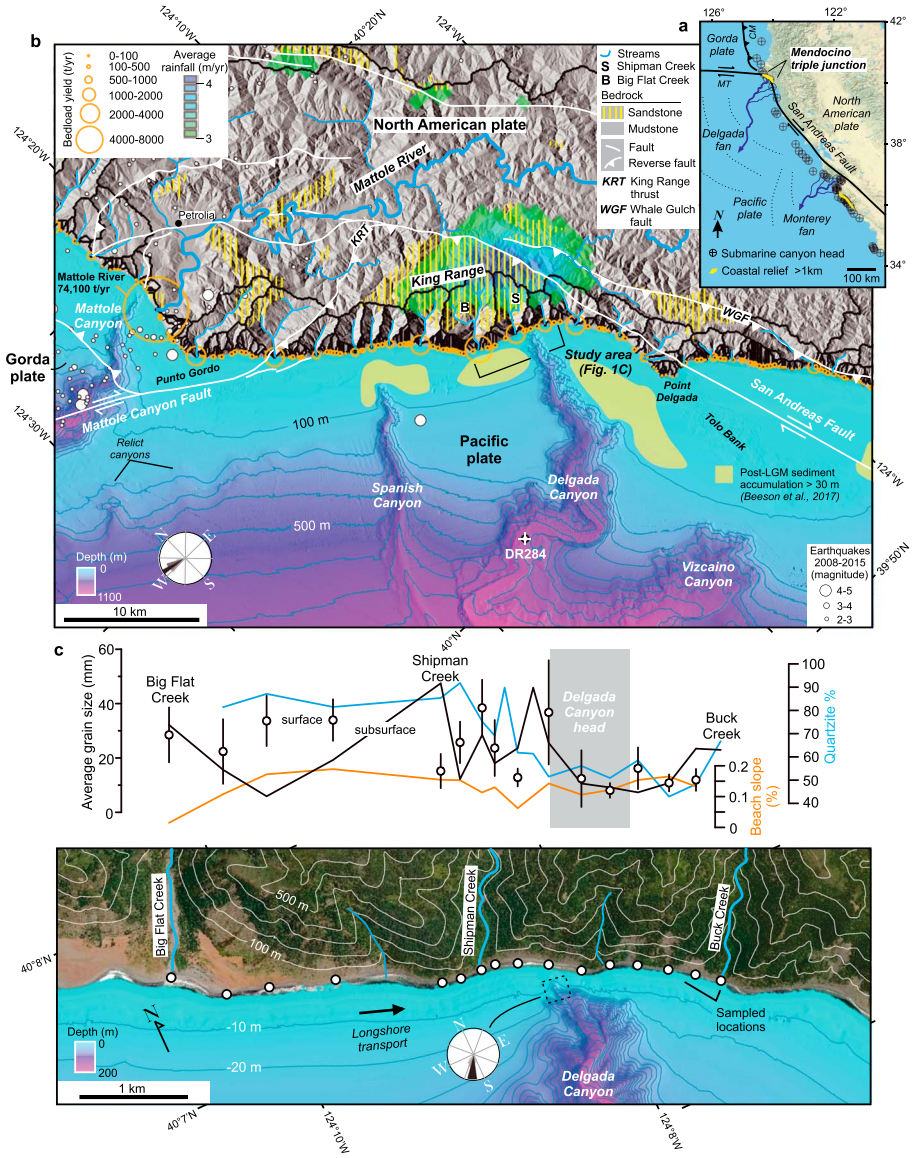


**Figure 1.** Delgada Canyon study area: (a) tectonic setting of the Mendocino triple junction in Northern California; (b) map of King Range and adjacent ocean showing faults, hydrology, bedrock lithology, offshore sediment thickness, and climate, adapted from McLaughlin et al. (2000) and Beeson et al. (2017). Wave rose (inset) compiled from data collected December 2016 to June 2018 by the Cape Mendocino buoy located at 40°17′41″N, 124°43′55″W (National Oceanic and Atmospheric Administration station 46213); (c) measured slope, grain size, and grain composition of beaches adjacent to Delgada Canyon. Wave rose for canyon head (inset) compiled from December 2016 to June 2018 Simulating WAves Nearshore model outputs (Figure 2b) rivers (Andrews & Antweiler, 2012), delivering on average 112,500 $m^3$/year of bed load to the coast. While Mattole River sediment is predominantly intercepted by Mattole Canyon, bedload delivered to the coast south of Punta Gordo is moved southeast by littoral currents toward Delgada Canyon (Patch & Griggs, 2006). Applying the bed load sediment model of Smith et al. (2017), which incorporates relief, bedrock composition, and PRISM-generated rainfall estimates (Figure 1b), creeks entering the Spanish Flats littoral cell updrift of Delgada Canyon contribute on average 103,900 $m^3$/year of bed load. Assuming a 5-to-1 suspended load to bedload proportion (Mueller & Pitlick, 2013), this would translate to 519,500 $m^3$/year total sediment budget for the littoral cell, comparable in magnitude to estimates of littoral transport in other coastal California settings. In comparison, 250,000 $m^3$/year of sediment transport is estimated to pass above Monterey Canyon (Best et al., 1991), and as much as 2,000,000 $m^3$/year of sediment moves through the Santa Barbara littoral cell above Hueneme and Mugu submarine canyons (Patch & Griggs, 2006). Seismic reflection surveys (Beeson et al., 2017) document that approximately 3 $km^3$ of sediment have accumulated on the shelf adjacent to Delgada Canyon since the end of the Last Glacial Maximum at ca. 18 kyr (Clark et al., 2009). This volume represents less than 6,000 years of the modeled littoral sediment supply for the Spanish Flats littoral cell, suggesting a substantial proportion this sediment exits the continental shelf through the Delgada Canyon.

Mendocino transform fault along a broad suite of reverse and strike slip faults (Figure 1b). Northward translation of the Pacific plate relative to the North American plate, estimated at 40 mm/year in Northern California, causes frequent earthquakes locally (Beeson et al., 2017; Freymueller et al., 1999). The Miocene King Range terrane that underlies the study area is a structural mélange of tightly folded argillite and well-compacted arkosic to volcanic-lithic sandstone *quartzite* bodies of varying thickness and aerial extent and is the westernmost and youngest portion of the Coastal belt of the Franciscan Complex (McLaughlin et al., 1982; McLaughlin et al., 2000). Coastal terraces suggest very rapid uplift (~4 mm/year) of the King Range during the latest Quaternary (Merritts, 1996; Merritts & Bull, 1989; Perron & Royden, 2013). Coastal catchments are steep and exhibit channel braiding and coarse flood debris suggesting large sediment loads (Snyder et al., 2003). According to the PRISM model (PRISM Climate Group, Oregon State University, http://prism.oregonstate.edu), the King Range receives nearly twice the annual precipitation as the gage at Petrolia, CA, due to topography (Figure 1b and supporting information Figure S1a).

The Spanish Flat littoral cell (Patch & Griggs, 2006) transports sediment predominantly eastward toward the Delgada Canyon headwall (Figure 1b). Beaches along this region are steep and reflective without a pronounced sandy low-tide terrace, typical of its energetic mesotidal setting with a large supply of coarse sediment (Buscombe & Masselink, 2006). Delgada Canyon trends roughly northeast to southwest across the continental slope, terminating at the Delgada deep-sea fan (Normark & Gutmacher, 1984; Figure 1a). Its most landward channel begins ~100 m from shore at 9-m depth (Figure 1c). At ~140-m depth, the steep (~13°) uppermost channels of Delgada Canyon amalgamate into a single sinuous bedrock channel with a ~5° slope, much steeper than the local continental shelf (~1.3°). Numerous tributary canyons join with Delgada canyon (Figure 2), including Spanish Canyon (Figure 1b), but the headwalls of these canyon are significantly below the depth of closure, implying disconnection from littoral sediment (Normark et al., 2009).

Coastal streams and bluff erosion provide abundant coarse sediment to the littoral cell updrift of the Delgada Canyon head (Figure 1b). While sediment yield from coastal creeks was not monitored, a sediment gage on the Mattole River, which drains the landward side of the King Range (Figure 1b), offers a useful comparison (Andrews & Antweiler, 2012). Its catchment delivers the second largest bed load (>1 mm) yield (3,100 t/km$^2$/year) of California rivers (Andrews & Antweiler, 2012), delivering on average 112,500 m$^3$/year of bed load to the coast. While Mattole River sediment is predominantly intercepted by Mattole Canyon, bedload delivered to the coast south of Punta Gordo is moved southeast by littoral currents toward Delgada Canyon (Patch & Griggs, 2006). Applying the bed load sediment model of Smith et al. (2017), which incorporates relief, bedrock composition, and PRISM-generated rainfall estimates (Figure 1b), creeks entering the Spanish Flats littoral cell updrift of Delgada Canyon contribute on average 103,900 m$^3$/year of bed load. Assuming a 5-to-1 suspended load to bedload proportion (Mueller & Pitlick, 2013), this would translate to 519,500-m$^3$/year total sediment budget for the littoral cell, comparable in magnitude to estimates of littoral transport in other coastal California settings. In comparison, 250,000 m$^3$/year of sediment transport is estimated to pass above Monterey Canyon (Best et al., 1991), and as much as 2,000,000 m$^3$/year of sediment moves through the Santa Barbara littoral cell above Hueneme and Mugu submarine canyons (Patch & Griggs, 2006). Seismic reflection surveys (Beeson et al., 2017) document that approximately 3 km$^3$ of sediment have accumulated on the shelf adjacent to Delgada Canyon since the end of the Last Glacial Maximum (LGM) at ca. 18 kyr (Clark et al., 2009). This volume represents less than 6,000 years of the modeled littoral sediment supply for the Spanish Flats littoral cell, suggesting that a substantial proportion of this sediment exits the continental shelf through the Delgada Canyon.

In this contribution, we hypothesize that littoral transport supplies Delgada Canyon with coarse sediment and that canyon focusing of wave energy into headwall gullies mobilizes coarse debris and triggers turbidity currents that incise its active axial channel. We apply repeat bathymetric surveys, grain size and provenance analysis, numerical wave modeling, and submarine channel network analysis to test this hypothesis.

## 2. Materials and Methods

### 2.1. Sonar Surveys

We surveyed the uppermost Delgada canyon region to the 240-m mean lower low water isobath using a Norbit multibeam sonar unit operating at 200 or 400 kHz (depending on water depth), in July of 2015 (see supporting information Text S1 for survey details). The resulting bathymetric map was compared with an

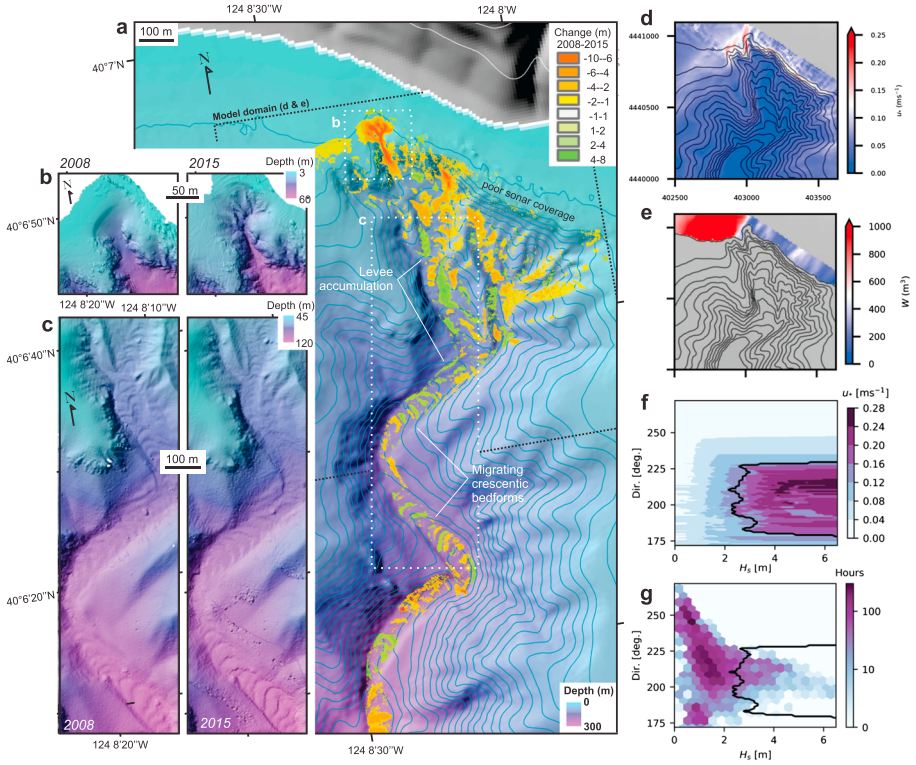


**Figure 2.** Repeat bathymetric surveys and wave modeling of Delgada canyon: (a) bathymetric change; (b) headwall detail; (c) channel detail; (d) estimated bed shear velocity, $u^*$, over the Simulating WAves Nearshore (SWAN) model domain, averaged over the period 30 December 2016 to 6 June 2018; (d) alongshore wave power, $W$, was computed in the nearshore region of the SWAN model domain up to the 10-m isobath; (e) derived from SWAN model outputs on a typical winter day (16 January 2018) with offshore (SWAN model boundary conditions provided by a regional Wavewatch III model) wave height, period, and direction of 4.3 m, 17.6 s, and 291°, respectively. The corresponding maps of $H_{rms}$ and ?$_{br}$ provided in supporting information Figure S2a and S2b, respectively; (f) distribution of modeled shear velocity, $u^*$, as a function of modeled wave direction and significant wave height, aggregated over the Delgada canyon headwall region (Figure 2b) over the period 30 December 2016 to 6 June 2018; (g) binned modeled wave direction and significant wave height, aggregated over headwall region (Figure 2b) over the same period, showing the distribution of the parameter space in time (number of hours). The black contour in panels f and g delimits the critical shear velocity for $D_{50}$ = 37 mm.

earlier survey conducted in 2008 by the California Seafloor Mapping Project (https://walrus.wr.usgs.gov/mapping/csmp) to reveal changes within and adjacent to the canyon head and in the canyon's axial channel (Figure 2 and supporting information Figure S3).

### 2.2. Sediment Grain Size and Provenance

Grain size, sediment composition, and beach morphology were measured at 16 locations during the summer of 2016 (Figure 1c and supporting information Figures S4 and S5). At each site, photos were taken of surface sediment along a shore-orthogonal transect for digital grain size analysis, following Warrick et al. (2009).

The wavelet method of Buscombe (2013) was used to estimate the grain size distribution from each photograph. Physical samples were collected within each transect for grain size and provenance analysis. Larger clasts were characterized in the field and a subsample of the smaller material ($\leq$22.6 mm) was sieved into half-phi increments and point counted for lithologic composition (Figure 1c). The Monterey Bay Aquarium Research Institute extracted two sediment cores from the channel of Delgada canyon at 861- and 864-m water depths in January 2013 (Figure 1b). These sediment cores both contain thin coarse sand intervals interpreted to represent deposition from recent turbidity currents, which are interbedded with hemipelagic mudstone (Figure 3a). A wood fragment in the uppermost turbidite in core VC-157 yielded a $>$ modern $^{14}$C date (supporting information Table S1), suggesting recent deposition.

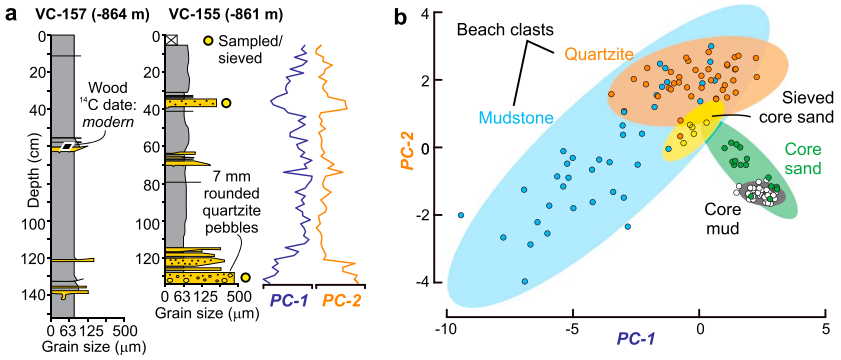


**Figure 3.** Sedimentary provenance: (a) stratigraphy and composition of sediment cores of the Delgada canyon thalweg (Figure 1b); (b) principal components of portable X-ray fluorescence-measured element concentrations, showing similarity between beach clasts and sand from recent turbidites that were cored at 861-m water depth. Two principal components account for 72% of the overall variance: PC-1 is correlated with lesser Fe, Al, K, Ti, and Ba concentrations; PC-2 is correlated with greater Si and Sr concentrations (cf. supporting information Table S2). Ellipses show 95% of the variation in the data.

Beach clasts and core materials were analyzed for 15 elements using a Niton XL3t 955 portable X-ray fluorescence (pXRF) device for comparison to core sediment. Sediment compositions are compared using principal component analysis, which transforms multiple correlated variables into a smaller number of uncorrelated variables, or principal components (Figure 3b; cf. supporting information Table S2), useful for sediment fingerprinting (e.g., Vale et al., 2016). Core VC-155 was measured at 5-cm increments using pXRF, and subsamples of the two sand intervals were sieved and washed in deionized water prior to analysis to remove interstitial mud, which represents less than 10% of the sand intervals, but coats larger particles.

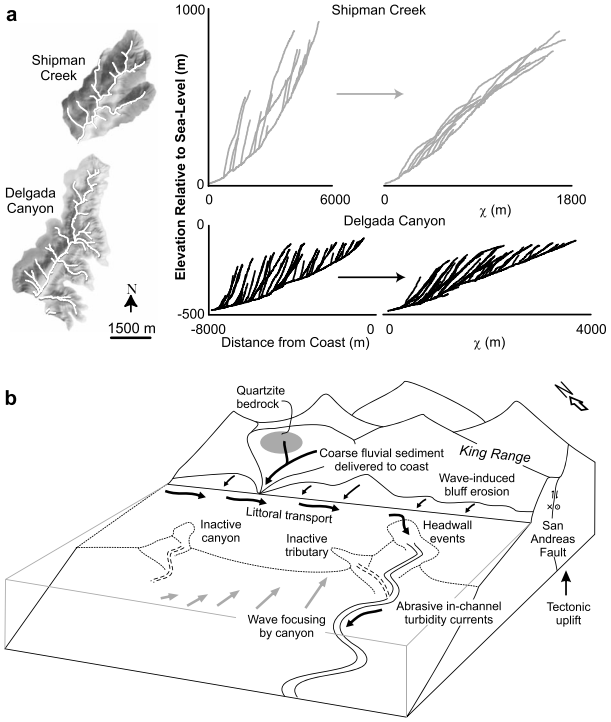


**Figure 4.** Incision of Delgada Canyon; (a) Chi transformation of Shipman Creek and Delgada canyon tributary networks; best fitting concavities are ~1/3 for Delgada canyon and ~½ for Shipman Creek; (b) process linkages between tectonic uplift-derived coarse sediment supply and canyon focusing of wave energy work to maintain canyon connectivity to shore in areas of rapid tectonic uplift.

### 2.3. Wave Modeling

Submarine canyon morphology has been shown to focus wave energy against coastlines (Long & Özkan-Haller, 2005). To better understand the influence of waves in the Delgada headwall region, we conducted wave modeling to study the influence of bottom topography on wave energy delivered to the bed in the headwall. The Simulating WAves Nearshore wave model (Booij et al., 1999; Zijlema, 2010; Zijlema & van der Westhuysen, 2005) was used to compute the wavefield in the coastal waters in the vicinity of Delgada canyon, every 3 hr for the period 30 December 2016 to 6 June 2018 (Figure 2 and supporting information Figure S2). Simulating WAves Nearshore models the spectral evolution of energy as waves propagate toward shore and has been used previously to simulate wavefields over complex topography, including submarine canyons (e.g., Gorrell et al., 2011; Rogers et al., 2007). Alongshore wave power was computed according to van Rijn (2014) as $W = H_{br}{}^{3}\sin\theta_{br}$ where $H_{br}$ and $\theta_{br}$ are, respectively, root-mean-square wave height and direction relative to shore, at wave breaking. We adopt a conventional parametric approach to predicting wave height at wave breaking as $H_{br} = \gamma H$, where $H$ is the root-mean-square shoaling wave height and $\gamma$ is the breaker depth index (e.g., Goda, 1970). Following Camenen and Larson (2007), we use $\gamma = 0.7$. van Rijn (2014) shows that alongshore sediment transport of gravel, and sand-gravel mixtures, is proportional to $W$. For more details see supporting information Text S2 (Eldeberky & Battjes, 1996; Rogers et al., 2003; Tolman & Chalikov, 1996; Wu, 1982; Zijlema & van der Westhuysen, 2005).

### 2.4. Channel Networks Analysis

Theory (Sklar & Dietrich, 2004, 2008) and field observations (Cook et al., 2012; Duvall et al., 2004; Finnegan et al., 2017; Johnson et al., 2009) show that the size and supply of coarse sediment strongly influence the efficiency of bedrock incision of fluvial channels. To test the role of coarse sediment in the incision of submarine canyons, we analyze the differences in the longitudinal profiles of adjacent submarine and river channel networks. Although both submarine and river canyons have dendritic channel networks, coarse sediment is input from hillslopes along the whole channel network in a river catchment, whereas coarse sediment in submarine systems is dominantly derived from regions coupled to the littoral supply. Consequently, because most submarine tributary heads were cut off from littoral sediment by sea level rise after the LGM (Normark et al., 2009), these currently *inactive* canyons transport no coarse sediment and must erode through different processes than *active* canyons. Submarine canyon profiles tend to be concave-up like those of rivers, although the reason is not well understood (Mitchell, 2005). In river networks, the scaling of slope and drainage area provides useful tools for distinguishing different process regimes (e.g., Stock & Dietrich, 2003) or regions with different sediment supplies (Finnegan et al., 2017; Johnson et al., 2009).

As a test of whether a signature of coarse sediment is apparent in the morphology of Delgada Canyon, we applied a *Chi transformation* to Delgada Canyon and Shipman Creek, the nearest terrestrial drainage to the head of Delgada Canyon. This removes the correlation between drainage area and slope that is inherent to all concave fluvial channels (Perron & Royden, 2013). If the transformed profile is linear and the tributaries and mainstem become collinear, we may infer that they operate via similar processes (e.g., Perron & Royden, 2013, Shelef & Hilley, 2014). The concept of drainage area does not apply to submarine systems, so for the analysis described below we define the upstream limit of the submarine channel network of Delgada Canyon where the active channel and tributary channel heads meet the shelf.

## 3. Results

### 3.1. Bathymetric Surveys

Comparison of repeat bathymetric surveys of Delgada Canyon in fall of 2008 and summer 2015 reveals that a large volume of sediment has been transported from the headwall (supporting information Figure S3). At the canyon's most landward channel, approximately 37,500 $m^3$ of sediment was removed from a 90-m-wide trough floored by several wave-aligned gullies that previously were occupied by a sediment shoal (Figure 2b). This channel merges with a 670-m-wide headwall that is drained by multiple steep channels, some of which contain migratory crescentic bedforms with 10- to 20-m wavelengths. Crescentic bedforms occur in as shallow as 30-m depth in the most landward channel (Figure 2b). At 140-m depth, several tributary channels consolidate into a single sinuous channel floored by 25- to 35-m wavelength crescentic bedforms (Figure 2c and supporting information Figure S3). Geomorphic change in the upper canyon head is

predominantly erosional, whereas the canyon's sinuous axial channel down to at least 240-m water depth contains alternating ~100-m-long reaches of net sediment accumulation and net erosion.

### 3.2. Provenance

The grain size and composition of beach sediment above the canyon head are strongly influenced by the bedrock geology of shore-draining catchments (Figure 1b). Coarse quartzite clasts are delivered by creeks that drain the central core of the range and mix with finer-grained mudstone clasts that originate from erosion of sea cliffs and bluffs. Quartzite clasts consequently must transit 0.6 km of the Spanish Flats littoral cell from the mouth of Shipman Creek to the head of Delgada Canyon. Beaches updrift of Delgada canyon are coarse grained and dominated by quartzite clasts (Figure 1c and supporting information Figure S4). Downshore past the Delgada Canyon headwall, the quartzite clast proportion decreases from 85% to 45% (Figure 1c and supporting information Figure S5). A coarse turbidite at the base of the VC-155 core contains rounded quartzite clasts that resemble clasts in the littoral zone upshore from the canyon headwall (Figure 3a). This finding is supported by pXRF measurements, which show that washed core sand closely resembles the average composition of beach clasts collected above the Delgada canyon head but differs significantly from the hemipelagic core mud (Figure 3). This difference in composition could reflect grain size-influenced mineralogic differences, or alternatively, a different source region for hemipelagic mud.

### 3.3. Wave Modeling

Shear stresses in the canyon headwall region are high due to significant focusing by refraction, in areas that coincide with maximum measured erosion during the surveyed interval (Figure 2d). Refraction attenuates wave energy, resulting in sheltering of littoral cell above the canyon head from longshore transport (Figure 2e). Refraction also makes the waves reach the vicinity of the canyon headwall faster than they otherwise would, traveling over a shorter fetch of dissipating continental shelf, and makes them align with the axis of the canyon to a greater degree. The result is that the waves have a greater tendency to hit the canyon headwall head on. We used a median size of 37 mm and arithmetic standard deviation (sorting coefficient) of 29 mm in the vicinity of the Delgada Canyon head (Figure 1c) to compute the fractional sediment mobilization threshold (critical shear stress) according to the formula of Buscombe and Conley (2012), which includes hiding/sheltering effects appropriate for sand and gravel mixtures. This mobilization threshold for the median grain size was likely exceeded over a wide range of conditions where significant wave height exceeded approximately 2.5 m at acute wave incidences (Figure 2f). An analysis of the total number of hours during which the critical shear stress for mobilizing the median grain size revealed that a narrow range of wave incidence (between 190° and 220°) is disproportionately important for sediment transport (Figure 2g). At this relatively shore-normal wave incidence, the canyon focuses waves into the region of the headwall that experienced greatest scour and shelters the nearshore region in the lee of the canyon from longshore current.

### 3.4. Channel Network Analysis

Network analysis of Shipman Creek and Delgada canyon reveals that the tributaries and mainstem of Shipman Creek have similar concavities and collapse onto essentially a single line, but in Delgada Canyon, the active mainstem and inactive tributaries cannot be fit with a single scaling relationship (Figure 3a). Specifically, it appears that the axial channel of Delgada Canyon exists at a shallower slope for a given upstream accumulated area than its tributaries.

## 4. Discussion

### 4.1. Sediment Transport Into Delgada Canyon

Repeat surveys of Delgada Canyon show that it collects littoral sediment derived from the rapidly uplifting King Range and periodically discharges this sediment downward into the canyon (Figure 2). Considering the predicted sediment budget for the Spanish Flats littoral cell, many transport events likely occurred during the surveyed interval, resulting ultimately in deep incision of a gully at the canyon head and migration of crescent-shaped bedforms characteristic of supercritical flow conditions at the bases of a coarse-grained turbidity currents (Covault et al., 2017; Hage et al., 2018). Due to the canyon's distance from the outlet of a major stream, these events were unlikely to have been triggered by river-generated hyperpycnal currents (Mulder et al., 2003) or plume settling at a river outlet (Hizzett et al., 2018). Instead, wave modeling

suggests that a strong longshore current ends abruptly above the canyon head due to canyon-induced sheltering, trapping, and temporarily accumulating sediment in the canyon headwall region. We infer from coincident maxima in geomorphic change and modeled shear stresses that a substantial proportion of sediment mobilization in Delgada Canyon is generated by waves in the uppermost canyon head (Figure 2d). This is consistent with the morphology of the uppermost canyon head, which resembles other wave-generated coastal-littoral landforms, including *geos*, littoral caves, and spur-and-groove reef topography (Blanco-Chao et al., 2007; Storlazzi et al., 2003; Trenhaile, 2016).

Based on analogy with other submarine canyons (Inman et al., 1976; Maier et al., 2018; Talling, 2014), and the historical record (supporting information Figure S1) and wave modeling, we infer that sediment is mobilized in the Delgada canyon head when wave agitation forms a suspension that collapses into a turbidity currents in a manner analogous to the river-generated plumes observed at the Squamish River delta in British Columbia (Hizzett et al., 2018). Turbidity currents are also likely triggered by landslides and/or breaching of loose sediment delivered by the littoral cell (Clare et al., 2016; Densmore et al., 1997; Mastbergen & van den Berg, 2003).

The sediment budget for Delgada Canyon should exert a fundamental control on the frequency of headwall sediment transport events and depends significantly on the proportion of material that bypasses canyon and is transported offshore to the shelf. Plausible scenarios yield event frequency estimates that vary significantly. Taking a typical assumption that 90% of the littoral sediment supply is transported offshore to the shelf (Limber et al., 2008), there is still enough sediment remaining in the littoral cell to recharge the canyon's uppermost gully approximately 10 times during the surveyed interval, on average one to two times per year. Alternatively, because measured post-LGM sediment volumes on the shelf offshore of the King Range (Beeson et al., 2017) represent less than a third of the post-LGM sediment budget (Figure 2b), a 90% bypass of fine sediment to the shelf seems unlikely, implying that transport events are significantly more common.

### 4.2. Submarine Bedrock Incision

We interpret the difference in slope scaling between the mainstem of Delgada Canyon and inactive tributary canyons to be a signature of coarse bedload in the mainstem of Delgada Canyon and its absence in currently inactive tributary canyons. This could reflect greater efficacy of channel incision when coarse sediment is present. Alternatively, from a transient perspective, this could reflect greater slope relaxation along the main stem, where a wave of incision has already passed, relative to tributaries, where knickpoints are still propagating landward (e.g., Johnson et al., 2009). The Chi analysis suggests that the Delgada canyon mainstem is actively carved into bedrock by turbidity currents generated at the Delgada canyon headwall (Figure 3a), and its close proximity to shore suggests that it has maintained connectivity to the littoral cell, presumably through headward erosion. Incision of the mainstem channel is likely accomplished by abrasion at the base of coarse turbidity currents energetic enough to mobilize the bed (Fildani et al., 2013; Sequeiros et al., 2010). Headward erosion of the uppermost canyon head by turbidity currents is less plausible, however, because such flows have little vertical space to accelerate at such shallow depths. Crescentic bedforms diagnostic of turbidity currents only appear below 30-m water depth. We infer from wave modeling and observed geomorphic changes and erosional forms that a substantial proportion of headward erosion of Delgada canyon is accomplished through wave driven scouring by coarse-grained sediment, rather than abrasion by turbidity currents.

### 4.3. Are Submarine Canyons Attracted to Shore?

Shepard and Emery (1941) noted that the largest submarine canyons offshore California are clustered around three mountainous coastal promontories (cf. Figure 1a) but did not specify the mechanism(s) responsible for this correspondence. Several classifications have been proposed for submarine canyon littoral connectivity (Romans et al., 2016; Sweet & Blum, 2016); however, no single mechanism has been identified to explain why a select group have avoided being disconnected during post-LGM sea level rise. Findings from Delgada Canyon may help explain these phenomena by showing that coarse sediment supply and wave focusing by submarine bathymetry work in concert to promote canyon incision and maintain littoral connectivity. The effectiveness of this mechanism is likely strongly modulated by the grain size and supply of clastic detritus in the system (Finnegan et al., 2017; Lamb et al., 2015; Sunamura, 2018), which is ultimately related to tectonic uplift and the presence of durable bedrock lithologies (Smith et al., 2017). We propose that high

littoral sediment supply and canyon focusing of waves make canyons *seek the shore* (Figure 3b). Seen through this lens, Delgada Canyon maintained connectivity during the post-LGM transgression because it intercepted coarse quartzite detritus from the central King Range, whereas nearby inactive Spanish Canyon was updrift from coarse sediment sources and did not incise into the shelf rapidly enough to maintain littoral connectivity (Figure 1b). These findings suggest canyons in other tectonically uplifting regions with durable terrestrial bedrock delivering coarse sediment to the shore should preferentially maintain connectivity to the shore.

## 5. Conclusions

Repeat bathymetry, provenance analysis, wave modeling, and channel network analysis indicate that wave energy is focused by the Delgada submarine canyon, promoting deposition of littoral sediment and inducing elevated wave shear stresses in its headwall region that frequently mobilize coarse bed material. We infer that abrasive turbidity currents generated from this process work to carve its active channel into bedrock. These findings highlight positive feedbacks between submarine canyons, waves, and sediment supply and suggests that submarine canyons adjacent to coarse sediment-rich, wave-dominated coastlines *seek the shore* and are more likely to persist during sea level highstands.

**Acknowledgments**
We thank C. Paull for initial suggestions, S. Neil for marine logistics, C. Sliva and M. Barton for field and laboratory assistance, R.J. Best for statistical advice, and K.L. Maier and B. Romans for insightful review comments. We thank the King Range Conservation Area, Seahorse Geomatics, the California Seafloor Mapping Project, USGS-Menlo Park sediment core laboratory, and Northern Arizona University and the Geological Society of America for funding. Bathymetric and XRF data may be accessed from https://figshare.com/s/ae31dae708db78cd7986. Cores were collected by Monterey Bay Aquarium Research Institute funded by the David and Lucile Packard Foundation.

## References

Andrews, E. D., & Antweiler, R. C. (2012). Sediment fluxes from California coastal rivers: The influences of climate, geology, and topography. *Journal of Geology*, *120*(4), 349–366. https://doi.org/10.1086/665733

Arzola, R. G., Wynn, R. B., Lastras, G., Masson, D. G., & Weaver, P. P. E. (2008). Sedimentary features and processes in the Nazaré and Setúbal submarine canyons, west Iberian margin. *Marine Geology*, *250*(1-2), 64–88. https://doi.org/10.1016/j.margeo.2007.12.006

Beeson, J. W., Johnson, S. Y., & Goldfinger, C. (2017). The transtensional offshore portion of the northern San Andreas fault: Fault zone geometry, late Pleistocene to Holocene sediment deposition, shallow deformation patterns, and asymmetric basin growth. *Geosphere*, *13*, 1173–1206.

Best, T. C., Griggs, G. B., & Osborne, R. H. (1991). A sediment budget for the Santa Cruz littoral cell, California. In R. H. Osborne (Ed.), *From shoreline to abyss; Contributions in marine geology in honor of Francis Parker Shepard*, edited by, (pp. 35–50). United States: SEPM (Society for Sedimentary Geology).

Blanco-Chao, R., Pérez-Alberti, A., Trenhaile, A. S., Costa-Casais, M., & Valcárcel, M. (2007). Shore platform abrasion in a para-periglacial environment, Galicia, northwestern Spain. *Geomorphology*. https://doi.org/10.1016/j.geomorph.2006.06.028

Booij, N., Ris, R. C., & Holthuijsen, L. H. (1999). A third-generation wave model for coastal regions, Part I. Model description and validation. *Journal of Geophysical Research*, *104*, 7649–7666. https://doi.org/10.1029/98JC02622

Buscombe, D. (2013). Transferable wavelet method for grain-size distribution from images of sediment surfaces and thin sections, and other natural granular patterns. *Sedimentology*, *60*(7), 1709–1732. https://doi.org/10.1111/sed.12049

Buscombe, D., & Conley, D. C. (2012). Effective shear stress of graded sediments. *Water Resources Research*, *48*, W05506. https://doi.org/10.1029/2010WR010341

Buscombe, D., & Masselink, G. (2006). Concepts in gravel beach dynamics. *Earth-Science Reviews*, *79*(1-2), 33–52. https://doi.org/10.1016/j.earscirev.2006.06.003

Camenen, B., & Larson, M. (2007). Predictive formulas for breaker depth index and breaker type. *Journal of Coastal Research*, *23*, 1028–1041.

Clare, M. A., Hughes Clarke, J. E., Talling, P. J., Cartigny, M. J. B., & Pratomo, D. G. (2016). Preconditioning and triggering of offshore slope failures and turbidity currents revealed by most detailed monitoring yet at a fjord-head delta. *Earth and Planetary Science Letters*, *450*, 208–220. https://doi.org/10.1016/j.epsl.2016.06.021

Clark, P. U., Dyke, A. S., Shakun, J. D., Carlson, A. E., Clark, J., Wohlfarth, B., et al. (2009). The Last Glacial Maximum. *Science*, *325*(5941), 710–714. https://doi.org/10.1126/science.1172873

Cook, K. L., Turowski, J. M., & Hovius, N. (2012). A demonstration of the importance of bedload transport for fluvial bedrock erosion and knickpoint propagation. *Earth Surface Processes and Landforms*, *38*, 683–695.

Covault, J. A., Kostic, S., Paull, C. K., Ryan, H. F., & Fildani, A. (2014). Submarine channel initiation, filling and maintenance from sea-floor geomorphology and morphodynamic modelling of cyclic steps. *Sedimentology*, *61*(4), 1031–1054. https://doi.org/10.1111/sed.12084

Covault, J. A., Kostic, S., Paull, C. K., Sylvester, Z., & Fildani, A. (2017). Cyclic steps and related supercritical bedforms: Building blocks of deep-water depositional systems, western North America. *Marine Geology*, 4–20.

Covault, J. A., Romans, B. W., Graham, S. A., Fildani, A., & Hilley, G. E. (2011). Terrestrial source to deep-sea sink sediment budgets at high and low sea levels: Insights from tectonically active Southern California. *Geology*, *39*(7), 619–622. https://doi.org/10.1130/G31801.1

Densmore, A. L., Anderson, R. S., McAdoo, B. G., & Ellis, M. A. (1997). Hillslope erosion by bedrock landslides. *Science*, *275*(5298), 369–372. https://doi.org/10.1126/science.275.5298.369

Dickinson, W. R., & Snyder, W. S. (1979). Geometry of triple junctions related to San Andreas transform. *Journal of Geophysical Research*, *84*(B2), 561–572. https://doi.org/10.1029/JB084iB02p00561

Duvall, A., Kirby, E., & Burbank, D. W. (2004). Tectonic and lithologic controls on bedrock channel profiles and processes in coastal California. *Journal of Geophysical Research*, *109*, F03002. https://doi.org/10.1029/2003JF000086

Eldeberky, Y., & Battjes, J. A. (1996). Spectral modeling of wave breaking: Application to Boussinesq equations. *Journal of Geophysical Research*, *101*(C1), 1253–1264. https://doi.org/10.1029/95JC03219

Fildani, A., Hubbard, S. M., Covault, J. A., Maier, K. L., Romans, B. W., Traer, M., & Rowland, J. C. (2013). Erosion at inception of deep-sea channels. *Marine and Petroleum Geology*, *41*, 48–61. https://doi.org/10.1016/j.marpetgeo.2012.03.006

Finnegan, N. J., Klier, R. A., Johnstone, S., Pfeiffer, A. M., & Johnson, K. (2017). Field evidence for the control of grain size and sediment supply on steady-state bedrock river channel slopes in a tectonically active setting. *Earth Surface Processes and Landforms*, *42*(14), 2338–2349. https://doi.org/10.1002/esp.4187

Freymueller, J. T., Murray, M. H., Segall, P., & Castillo, D. (1999). Kinematics of the Pacific-North America Plate Boundary Zone, Northern California. *Journal of Geophysical Research*, *104*(B4), 7419–7441. https://doi.org/10.1029/1998JB900118

Goda, Y. (1970). A synthesis of breaker indices. *Proceedings. Japan Society of Civil Engineers*, *1970*(180), 39–49. https://doi.org/10.2208/jscej1969.1970.180_39

Goldfinger, C., Morey, A. E., Nelson, C. H., Gutierrez-Pastor, J., Johnson, J. E., Karabanov, E., et al. (2007). Rupture lengths and temporal history of significant earthquakes on the offshore and north coast segments of the Northern San Andreas Fault based on turbidite stratigraphy. *Earth and Planetary Science Letters*, *254*(1-2), 9–27. https://doi.org/10.1016/j.epsl.2006.11.017

Gorrell, L., Raubenheimer, B., Elgar, S., & Guza, R. T. (2011). SWAN predictions of waves observed in shallow water onshore of complex bathymetry. *Coastal Engineering*, *58*(6), 510–516. https://doi.org/10.1016/j.coastaleng.2011.01.013

Hage, S., Cartigny, M. J. B., Clare, M. A., Sumner, E. J., Vendettuoli, D., Hughes Clarke, J. E., et al. (2018). How to recognize crescentic bedforms formed by supercritical turbidity currents in the geologic record: Insights from active submarine channels. *Geology [Boulder]*, *46*(6), 563–566. https://doi.org/10.1130/G40095.1

Hizzett, J. L., Hughes Clarke, J. E., Sumner, E. J., Cartigny, M. J. B., Talling, P. J., & Clare, M. A. (2018). Which triggers produce the most erosive, frequent, and longest runout turbidity currents on deltas? *Geophysical Research Letters*, *45*, 855–863. https://doi.org/10.1002/2017GL075751

Inman, D. L., Nordstrom, C. E., & Flick, R. E. (1976). Currents in submarine canyons; An air-sea-land interaction. *Annual Review of Fluid Mechanics*, *8*(1), 275–310. https://doi.org/10.1146/annurev.fl.08.010176.001423

Johnson, J. P. L., Whipple, K. X., Sklar, L. S., & Hanks, T. C. (2009). Transport slopes, sediment cover, and bedrock channel incision in the Henry Mountains, Utah. *Journal of Geophysical Research*, *114*, F02014. https://doi.org/10.1029/2007JF000862

Lamb, M. P., Finnegan, N. J., Scheingross, J. S., & Sklar, L. S. (2015). New insights into themechanics of fluvial bedrock erosion through flume experiments and theory. *Geomorphology*, *244*, 33–55. https://doi.org/10.1016/j.geomorph.2015.03.003

Limber, P. W., Patsch, K. B., & Griggs, G. B. (2008). Coastal sediment budgets and the littoral cutoff diameter: A grain size threshold for quantifying active sediment inputs. *Journal of Coastal Research*, *24*, 122–133.

Long, J. W., & Özkan-Haller, H. T. (2005). Offshore controls on nearshore rip currents. *Journal of Geophysical Research*, *110*, C12007. https://doi.org/10.1029/2005JC003018

Maier, K. L., Johnson, S. Y., & Hart, P. (2018). Controls on submarine canyon head evolution: Monterey Canyon, offshore central California. *Marine Geology*, *404*, 24–40.

Mastbergen, D. R., & van den Berg, J. H. (2003). Breaching in fine sands and the generation of sustained turbidity currents in submarine canyons. *Sedimentology*, *50*(4), 625–637. https://doi.org/10.1046/j.1365-3091.2003.00554.x

McLaughlin, R. J., Ellen, S. D., Blake, M. C., Jayco, A. S., Irwin, W. P., Aalto, R., et al. (2000). *Geology of the Cape Mendicino, Eureka, Garberville, and southwestern part of the Hayfork 30 × 60 minute quadrangles and adjacent offshore area*. U.S. Geological Survey: Northern California.

McLaughlin, R. J., Kling, S. A., Poore, R. Z., McDougall, K., & Beutner, E. C. (1982). Post-middle Miocene accretion of Franciscan rocks, northwestern California. *Geological Society of America Bulletin*, *93*(7), 595–605. https://doi.org/10.1130/0016-7606(1982)93<595:PMAOFR>2.0.CO;2

Merritts, D., & Bull, W. B. (1989). Interpreting Quaternary uplift rates at the Mendicino triple junction, Northern California, from uplifted marine terraces. *Geology*, *17*(11), 1020–1024. https://doi.org/10.1130/0091-7613(1989)017<1020:IQURAT>2.3.CO;2

Merritts, D. J. (1996). The Mendocino triple junction: Active faults, episodic coastal emergence, and rapid uplift. *Journal of Geophysical Research*, *101*(B3), 6051–6070. https://doi.org/10.1029/95JB01816

Mitchell, N. C. (2005). Interpreting long-profiles of canyons in the USA Atlantic continental slope. *Marine Geology*, *214*(1-3), 75–99. https://doi.org/10.1016/j.margeo.2004.09.005

Mitchell, N. C. (2014). Bedrock erosion by sedimentary flows in submarine canyons. *Geosphere*, *10*(5), 892–904. https://doi.org/10.1130/GES01008.1

Mueller, E. R., & Pitlick, J. (2013). Sediment supply and channel morphology in mountain river systems: 1. Relative importance of lithology, topography, and climate. *Journal of Geophysical Research: Earth Surface*, *118*, 2325–2342. https://doi.org/10.1002/2013JF002843

Mulder, T., Syvitski, J. P. M., Migeon, S., Faugères, J.-C., & Savoye, B. (2003). Marine hyperpycnal flows: Initiation, behavior and related deposits. A review. *Marine and Petroleum Geology*, *20*(6-8), 861–882. https://doi.org/10.1016/j.marpetgeo.2003.01.003

Normark, W. R., & Gutmacher, C. E. (1984). Delgada fan: Preliminary interpretation of channel development. *Geo-Marine Letters*, *3*, 79–83.

Normark, W. R., Piper, D. J. W., Romans, B. W., Covault, J. A., Dartnell, P., & Sliter, R. W. (2009). Submarine canyon and fan systems of the California continental borderland. In H. J. Lee & W. R. Normark (Eds.), *Earth science in the urban ocean; the Southern California continental borderland* (pp. 141–168). Boulder, CO: Geological Society of America. https://doi.org/10.1130/2009.2454(2.7)

Parker, G. (1982). Conditions for the ignition of catastrophically erosive turbidity currents. *Marine Geology*, *46*(3-4), 307–327. https://doi.org/10.1016/0025-3227(82)90086-X

Patch, K., & Griggs, G. (2006). *Littoral cells, sand budgets, and beaches: Understanding California's shoreline*. Santa Cruz: Institute of Marine Sciences, University of California.

Paull, C. K., Caress, D. W., Ussler, W. I., Lundsten, E., & Meiner-Johnson, M. (2011). High-resolution bathymetry of the axial channels within Monterey and Soquel submarine canyons, offshore central California. *Geosphere*, *7*, 1077–1101.

Paull, C. K., Ussler, W. I., Greene, H. G., Keaten, R., Mitts, P., & Barry, J. (2003). Caught in the act: The 20 December 2001 gravity flow event in Monterey Canyon. *Geo-Marine Letters*, *22*, 227–232.

Perg, L. A., Anderson, R. S., & Finkel, R. C. (2003). Use of cosmogenic nuclides as a sediment tracer in the Santa Cruz littoral cell, California, United States. *Geology*, *31*(4), 299–302. https://doi.org/10.1130/0091-7613(2003)031<0299:UOCRAA>2.0.CO;2

Perron, J. T., & Royden, L. (2013). An integral approach to bedrock river profile analysis. *Earth Surface Processes and Landforms*, *38*(6), 570–576. https://doi.org/10.1002/esp.3302

Rogers, W. E., Hwang, P. A., & Wang, D. W. (2003). Investigation of wave growth and decay in the SWAN model: Three regional-scale applications. *Journal of Physical Oceanography*, *33*(2), 366–389. https://doi.org/10.1175/1520-0485(2003)033<0366:IOWGAD>2.0.CO;2

Rogers, W. E., Kaihatu, J. M., Hsu, L., Jensen, R. E., Dykes, J. D., & Holland, K. T. (2007). Forecasting and hindcasting waves with the SWAN model in the Southern California Bight. *Coastal Engineering*, *54*(1), 1–15. https://doi.org/10.1016/j.coastaleng.2006.06.011

Romans, B. W., Castelltort, S., Covault, J. A., Fildani, A., & Walsh, J. P. (2016). Environmental signals propagation in sedimentary systems across timescales. *Earth-Science Reviews*, *153*, 7–29. https://doi.org/10.1016/j.earscirev.2015.07.012

Sequeiros, O. E., Spinewine, B., Beuaubouef, R. T., Sun, T., Garcia, M. H., & Parker, G. (2010). Bedload transport and bed resistance associated with density and turbidity currents. *Sedimentology*, *57*(6), 1463–1490. https://doi.org/10.1111/j.1365-3091.2010.01152.x

Shelef, E., & Hilley, G. E. (2014). Symmetry, randomness, and process in the structure of branched channel networks. *Geophysical Research Letters*, *41*, 3485–3493. https://doi.org/10.1002/2014GL059816

Shepard, F. P. (1981). Submarine canyons: Multiple causes and long term persistence. *American Association of Petroleum Geologists Bulletin*, *65*, 1062–1077.
Shepard, F. P., & Dill, R. F. (1966). *Submarine canyons and other sea valleys* (p. 381). Chicago: Rand McNally.
Shepard, F. P., & Emery, K. O. (1941). *Submarine topography off the California coast: Canyons and tectonic interpretation*, (Vol. 31, p. 171). Boulder: Geological Society of America Special Paper.
Sklar, L. S., & Dietrich, W. E. (2004). A mechanistic model for river incision into bedrock by saltating bed load. *Water Resources Research*, *40*, W06301. https://doi.org/10.1029/2003WR002496
Sklar, L. S., & Dietrich, W. E. (2008). Implications of the saltation-abrasion bedrock incision model for steady-state river longitudinal profile relief and concavity. *Earth Surface Processes and Landforms*, *33*(7), 1129–1151. https://doi.org/10.1002/esp.1689
Smith, M. E., Finnegan, N. J., Mueller, E. R., & Best, R. J. (2017). Durable terrestrial bedrock predicts submarine canyon formation. *Geophysical Research Letters*, *44*, 10,332–310,340. https://doi.org/10.1002/2017GL075139
Snyder, N. P., Whipple, K. X., Tucker, G. E., & Merritts, D. (2003). Channel response to tectonic forcing: Field analysis of stream morphology and hydrology in the Mendocino triple junction region, Northern California. *Geomorphology*, *53*(1-2), 97–127. https://doi.org/10.1016/S0169-555X(02)00349-5
Stock, J., & Dietrich, W. E. (2003). Valley incision by debris flows: Evidence of a topographic signature. *Water Resources Research*, *39*(4), 1089. https://doi.org/10.1029/2001WR001057
Storlazzi, C. D., Logan, J. B., & Field, M. E. (2003). Quantitative morphology of a fringing reef tract from high-resolution laser bathymetry: Southern Molokai, Hawaii. *GSA Bulletin*, *115*(11), 1344–1355. https://doi.org/10.1130/B25200.1
Sunamura, T. (2018). A fundamental equation for describing the rate of bedrock erosion by sediment-laden fluid flows in fluvial, coastal, and aeolian environments. *Earth Surface Processes and Landforms*. https://doi.org/10.1002/esp.4467
Sweet, M. L., & Blum, M. D. (2016). Connections between fluvial to shallow marine environments and submarine canyons: Implications for sediment transfer to deep water. *Journal of Sedimentary Research*, *86*(10), 1147–1162. https://doi.org/10.2110/jsr.2016.64
Talling, P. J. (2014). On the triggers, resulting flow types and frequencies of subaqueous sediment density flows in different settings. *Marine Geology*, *352*, 155–182. https://doi.org/10.1016/j.margeo.2014.02.006
Tolman, H. L., & Chalikov, D. (1996). Source terms in a third-generation wind wave model. *Journal of Physical Oceanography*, *26*(11), 2497–2518. https://doi.org/10.1175/1520-0485(1996)026<2497:STIATG>2.0.CO;2
Trenhaile, A. (2016). Rocky coasts—Their role as depositional environments. *Earth-Science Reviews*. https://doi.org/10.1016/j.earscirev.2016.05.001
Vale, S. S., Fuller, I. C., Procter, J. N., Basher, L. R., & Smith, I. E. (2016). Application of a confluence-based sediment-fingerprinting approach to a dynamic sedimentary catchment, New Zealand. *Hydrological Processes*, *30*(5), 812–829. https://doi.org/10.1002/hyp.10611
van Rijn, L. C. (2014). A simple general expression for longshore transport of sand, gravel and shingle. *Coastal Engineering*, *90*, 23–39. https://doi.org/10.1016/j.coastaleng.2014.04.008
Warrick, J. A., Rubin, D. M., Ruggiero, P., Harney, J. N., Draut, A. E., & Buscombe, D. (2009). Cobble cam: Grain-size measurements of sand to boulder from digital photographs and autocorrelation analyses. *Earth Surface Processes and Landforms*, *34*(13), 1811–1821. https://doi.org/10.1002/esp.1877
Wu, J. (1982). Wind-stress coefficients over sea surface from breeze to hurricane. *Journal of Geophysical Research*, *87*(C12), 9704–9706. https://doi.org/10.1029/JC087iC12p09704
Zijlema, M. (2010). Computation of wind-wave spectra in coastal waters with SWAN on unstructured grids. *Coastal Engineering*, *57*(3), 267–277. https://doi.org/10.1016/j.coastaleng.2009.10.011
Zijlema, M., & van der Westhuysen, A. J. (2005). On convergence behaviour and numerical accuracy in stationary SWAN simulations of nearshore wind wave spectra. *Coastal Engineering*, *52*(3), 237–256. https://doi.org/10.1016/j.coastaleng.2004.12.006